

## Insights into function of PSI domains from structure of the Met receptor PSI domain

Guennadi Kozlov<sup>a</sup>, Audrey Perreault<sup>b</sup>, Joseph D. Schrag<sup>b</sup>, Morag Park<sup>a</sup>,  
Miroslaw Cygler<sup>b</sup>, Kalle Gehring<sup>a</sup>, Irena Ekiel<sup>b,\*</sup>

<sup>a</sup> Department of Biochemistry, McGill University, 3655 Promenade Sir William Osler, Montréal, Que., Canada H3G 1Y6

<sup>b</sup> Health Sector, Biotechnology Research Institute, National Research Council of Canada, 6100 Royalmount Avenue, Montréal, Que., Canada H4P 2R2

Received 10 June 2004

### Abstract

PSI domains are cysteine-rich modules found in extracellular fragments of hundreds of signaling proteins, including plexins, semaphorins, integrins, and attractins. Here, we report the solution structure of the PSI domain from the human Met receptor, a receptor tyrosine kinase critical for proliferation, motility, and differentiation. The structure represents a cysteine knot with short regions of secondary structure including a three-stranded antiparallel  $\beta$ -sheet and two  $\alpha$ -helices. All eight cysteines are involved in disulfide bonds with the pattern consistent with that for the PSI domain from Sema4D. Comparison with the Sema4D structure identifies a structurally conserved core comprising the N-terminal half of the PSI domain. Interestingly, this part links adjacent SEMA and immunoglobulin domains in the Sema4D structure, suggesting that the PSI domain serves as a wedge between propeller and immunoglobulin domains and is responsible for the correct positioning of the ligand-binding site of the receptor. Crown Copyright © 2004 Published by Elsevier Inc. All rights reserved.

**Keywords:** PSI domain; Met receptor; HGF receptor; Cysteine-rich domain; NMR structure

The Met receptor belongs to a class of receptor tyrosine kinases critical for proliferation, motility, survival, and differentiation. Upon binding of Met to hepatocyte growth factor/scatter factor (HGF/SF), multiple proliferative and anti-apoptotic cellular responses are induced, often resulting in colony dispersal (scattering) and the epithelial to mesenchymal transition (reviewed in [1]). As in many other receptor tyrosine kinases, ligand binding leads to dimerization and autophosphorylation of the cytoplasmic kinase domain, resulting in recruitment of signaling mediators, such as Gab1 (for a review, see [2]). Met receptors are important in both normal development and malignancy. Dysregulation of Met in tumor cells leads to an invasive phenotype, which may result from simultaneous expression of Met and

HGF in tumor cells, overexpression of Met or mutations in its kinase domain [3]. Since HGF/Met signaling is crucial for invasion and metastasis, targeting these proteins may block the malignant process [4].

As most other receptors, Met has a modular structure. The ectodomain exposed on the cell surface has an N-terminal semaphorin (SEMA) domain, followed by the plexin, semaphorin, and integrin (PSI) domain, four immunoglobulin-like IPT domains, a transmembrane region, and cytosolic tyrosine kinase domain. The 3D structure of the SEMA domain of semaphorin was determined recently [5,6] and identifies this domain as having a 7-blade  $\beta$ -propeller fold. The SEMA domain is common to semaphorins, plexins, and Met-like receptors and may serve as a key element for ligand binding. The architecture of these receptors has common features in terms of additional domains in the extracellular part, such as EGF, IPT, or TSP domains [7]. They likely form

\* Corresponding author. Fax: +1-514-496-5143.  
E-mail address: [irena.ekiel@nrc.ca](mailto:irena.ekiel@nrc.ca) (I. Ekiel).

a stalk, reminiscent of that in integrins [8]. The PSI domain provides a link between the stalk and the propeller-like ligand recognition domain and can be present as a single copy or as multiple copies.

PSI domains constitute a large group of cysteine-rich modules present in extracellular fragments of over 500 signaling proteins [7]. The general functions of these proteins include cell guidance, scattering, differentiation, and pigmentation/body weight regulation. Other members of the rapidly growing group of PSI-containing proteins include the pituitary tumor-transforming gene (PTTG) interacting protein [9] and surface proteins ND7 and ND169 from *Paramecium tetraurelia* [10]. Mutations in the region comprising the PSI domain in semaphorin 3A modulate biological activity, indicating that this fragment is important for function [11]. PSI domains comprise three to four disulfides over approximately 50 amino acid residues. The only available structural information on the PSI domain comes from the Sema4D X-ray structure [6]. Although the PSI domain was present in the crystal structure of integrin [8,12], its corresponding electron density was weak and this domain was not included in the final model. The very recent structural study on the Met receptor [13] did not provide the detailed analysis of the PSI domain and the coordinates were not available at the moment of submission of this manuscript. The low sequence identity between the members of PSI family makes it essential to have several representative structures from this family to understand the level of structural divergence and to shed more light on the currently unknown function of this frequently occurring protein module. Additional structural data are also required to address the discrepancy in disulfide pairing derived from structural [6] and biochemical [14] experimental data.

In this work we investigated the solution structure of the PSI domain from the human Met receptor using nuclear magnetic resonance spectroscopy. Comparison of the structure with that of Sema4D identifies the structural core of the PSI domains, which interacts with the neighboring propeller and immunoglobulin-like domains. This suggests that the PSI domain functions as a linking module to orient the extracellular fragment of a receptor for proper ligand binding.

## Materials and methods

**Expression and purification of the PSI domain.** The PSI domain of the Met receptor (amino acids 519–562) was cloned into a modified pET32a vector (Novagen) and expressed as a fusion with thioredoxin using the *Escherichia coli* Origami strain (Novagen).  $^{15}\text{N}$ -labeled PSI domain was prepared using minimal medium enriched in  $^{15}\text{N}$ -labeled leucine, with  $^{15}\text{N}$ -ammonium sulfate as a primary source of nitrogen. Ni-NTA affinity chromatography was used for protein purification. The cleavage with thrombin produced a 48-residue protein including the N-terminal sequence Gly-Ser-Ala-Met from the vector. A second

pass through the Ni-NTA column resulted in pure and homogeneous PSI domain, as checked by reverse phase HPLC and SDS-PAGE electrophoresis under reducing and non-reducing conditions. The final yield of the soluble protein was 1–1.5 mg from 9 L of the rich medium. The identity of the protein was verified by mass spectrometry (Sciex electrospray). Free cysteines could not be detected using 5,5'-dithio-bis(2-nitro)benzoate (DTNB) assay, confirming that all cysteines are involved in disulfide formation.

**NMR spectroscopy.** NMR experiments (unless specified otherwise) were carried out at 283 K and pH 6.0, using a 1 mM PSI sample in 50 mM phosphate buffer, 0.15 M NaCl on a Bruker DRX500 spectrometer. Initial NMR spectra indicated that the protein was homogeneous and folded. Since the domain is very small (48 amino acid residues), and NMR signals are well dispersed, homonuclear 2D NMR experiments were sufficient for both resonance assignments and structure determination. Assignment of  $^1\text{H}$  resonances was achieved by standard procedures using a combination of 2D homonuclear TOCSY (110 ms mixing time) and NOESY (150 ms mixing time) experiments. Additional  $^1\text{H}$ ,  $^{15}\text{N}$ -HSQC was performed using  $^{15}\text{N}$ -enriched sample, to verify the assignment of specific signals. Natural abundance  $^1\text{H}$ ,  $^{13}\text{C}$ -HSQC experiments performed at 283 and 303 K using unlabeled sample confirmed that all cysteine residues are involved in disulfide bonds.  $^3J \text{H}^{\text{N}}\text{-H}^{\alpha}$  coupling constants were obtained from a DQF-COSY experiment. NMR spectra were processed using XWINNMR (Bruker Biospin) software and analyzed with XEASY [15].

**Structure calculations.** Structures were calculated using the CANDID module implemented in the program Cyana [16]. NOE restraints were obtained from 2D homonuclear NOESY experiments using samples containing 10% and 100%  $\text{D}_2\text{O}$ . 2D NOESY spectra were used with CANDID to calibrate and assign NOE cross-peaks. Automatically assigned long-ranged NOEs were manually checked to confirm the disulfide pairing. The 20 lowest-energy structures obtained after seven cycles of calculations in Cyana were further refined using standard protocols in Xplor-NIH [17] to yield the final ensemble. The quality of obtained structures was assessed using PROCHECK [18]. The Ramachandran plot generated for all final structures shows 94.6% residues in the most favored and allowed regions with only 0.1% in disallowed region. The structural statistics are shown in Table 1. Coordinates and NMR constraints were deposited with the Protein DataBank (<http://www.rcsb.org/pdb/>) under PDB ID code 1SSL.

Table 1  
Structural statistics for PSI domain

<i>Restraints for structure calculations</i>	
Total restraints used	492
Total NOE restraints	407
Intraresidual	125
Sequential ( $ i - j  = 1$ )	120
Medium range ( $1 <  i - j  < 5$ )	50
Long range ( $ i - j  \geq 5$ )	112
Hydrogen bond restraints	19
Dihedral angles restraints	66
<i>R.m.s. deviations from experimental restraints</i>	
Distance deviations (Å)	0.010 ± 0.0021
Dihedral deviations (°)	0.375 ± 0.0727
<i>Deviations from idealized geometry</i>	
Bonds (Å)	0.0021 ± 0.0001
Angles (°)	0.5687 ± 0.0094
Improper (°)	0.3955 ± 0.0114
<i>R.m.s. deviations of the 20 structures from the mean coordinates (Å)</i>	
Backbone (residues Cys520–Cys561)	0.52 ± 0.14
Heavy atoms (residues Cys520–Cys561)	0.98 ± 0.16

## Results

### Structure of the PSI domain

The structure of the PSI domain from the Met receptor represents a cysteine knot with short regions of regular secondary structure (Fig. 1). The secondary structure includes two N-terminal  $\alpha$ -helices (Cys520–Phe523 and Cys526–Ser531) positioned on the same side of a three-stranded antiparallel  $\beta$ -sheet of strands  $\beta$ 1 (Cys538–Cys541),  $\beta$ 2 (Lys544–Arg547), and  $\beta$ 3 (Trp 556–Gln558). The structure is stabilized by four disulfides Cys520–Cys538, Cys526–Cys561, Cys529–Cys545, and Cys541–Cys551 (Fig. 1C), which largely account for the hydrophobic core of the domain. Disulfide pairing resulting from the structure calculation is fully consistent with that found in the Sema4D X-ray structure [6] and differs from the one based on biochemical data

for integrins [14]. Despite the presence of eight cysteine residues, the Met PSI domain could be produced in *E. coli* with all four disulfides uniquely assembled; no other conformations were detected by NMR spectroscopy. This provides a strong indication that the disulfide pattern found in the PSI domain structure in this study and in Sema4D [6] is the only one that leads to a soluble and stable fold.

The structures of the PSI domains from the Met receptor and Sema4D explain sequence conservation observed for the PSI domains (Fig. 2). The sequence alignment is guided by the six invariant and two highly conserved cysteines. There is a significant variability in spacing between most of the cysteine residues. The only well-conserved spans are between cysteines 2 and 3 (C<sup>526</sup>SQC<sup>529</sup>) and 4 and 5 (C<sup>538</sup>GWC<sup>541</sup>). The latter is positioned in the middle of the domain resulting in a strong preference for a small amino acid (usually glycine

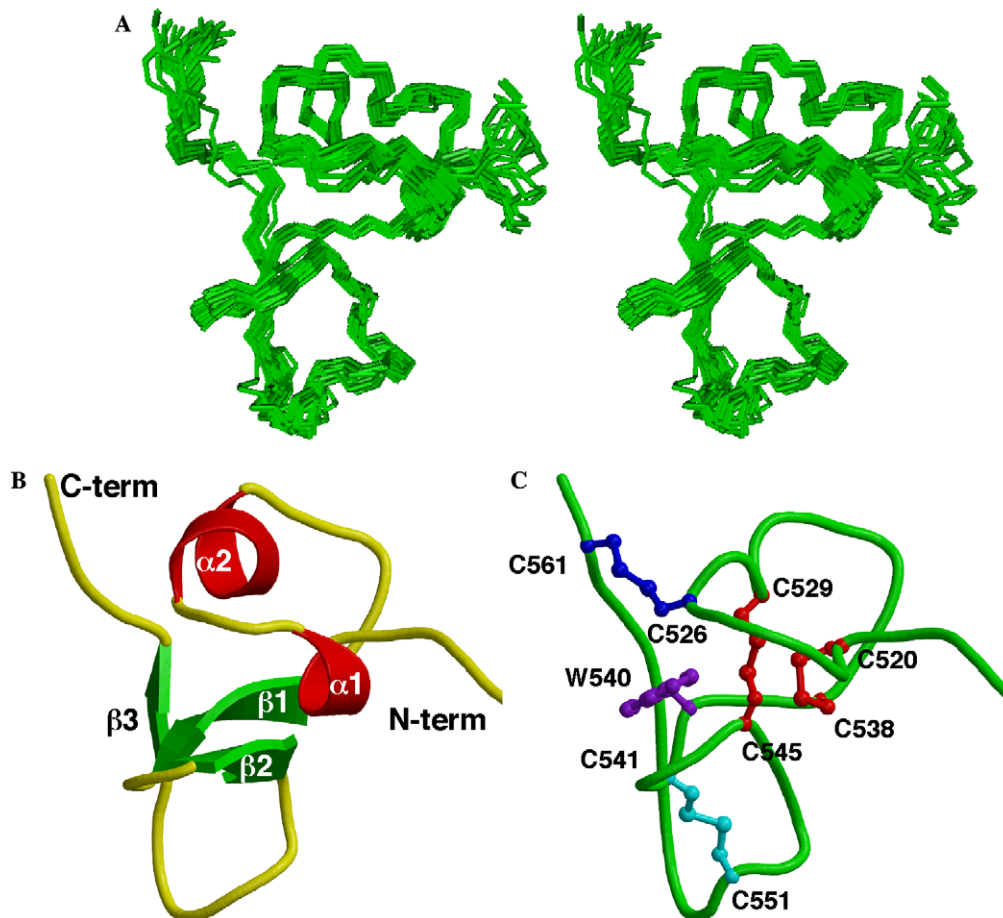


Fig. 1. Structure of the PSI domain from the Met receptor. (A) Stereo view of the backbone superposition of the 20 lowest-energy structures for residues Met518–Leu562 generated with MOLMOL [20]. (B) Ribbon representation of the lowest-energy PSI domain structure generated with MOLSCRIPT [21] and Raster3D [22]. The secondary structure elements and N- and C-termini are labeled. (C) Tube representation of the lowest-energy structure with disulfides explicitly shown. Two conserved disulfides (in red) stabilize the structural core of the domain, while the third one (in blue) orients the C-terminus. The remaining disulfide (in cyan) is dispensable. The side chain of the conserved Trp540 (in purple) is partially buried and may help in forming correct disulfide pairing. (For interpretation of the references to color in this figure legend, the reader is referred to the web version of this paper.)

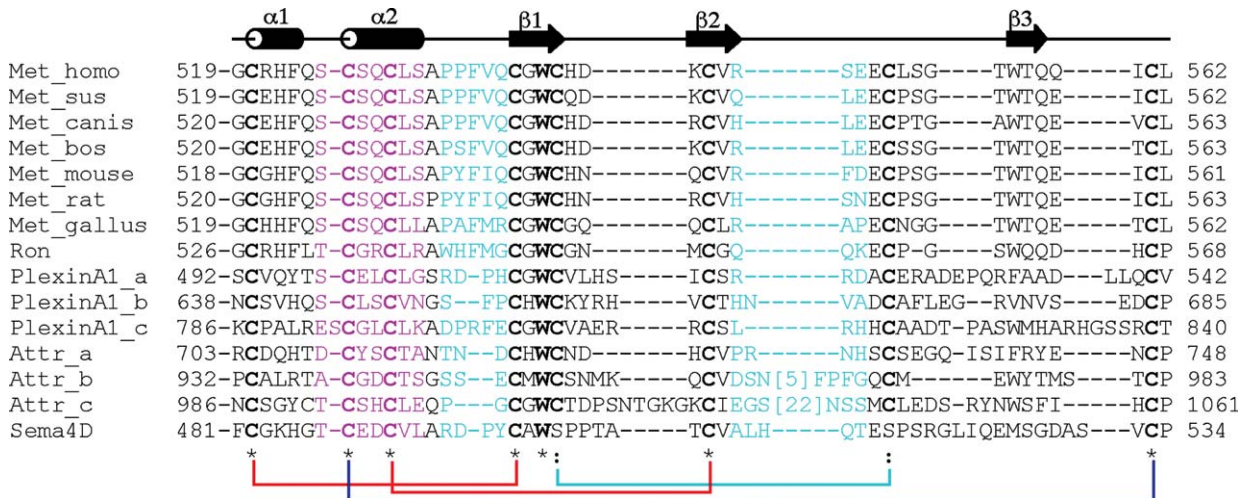


Fig. 2. The PSI domains show little sequence similarity besides the six conserved cysteines and the tryptophan residue (Trp540 in the human Met receptor). The aligned PSI domains are from human (Met\_homo, gi:66818), pig (Met\_sus, gi:38322750), dog (Met\_canis, gi:38322713), cow (Met\_bos, gi:38322702), mouse (Met\_mouse, gi:125485), rat (Met\_rat, gi:13629392), and chicken (Met\_gallus, gi:38322685) Met receptors, human Ron (gi:585912), and Sema4D (gi:37927181) receptors, and different PSI domains (labeled a, b, and c) from human plexin-A1 (gi:6010217) and attractin (Attr, gi:8118082). The conserved residues are in bold. The propeller domain-interacting regions (in cyan) and IG-like domain-interacting region (in purple) are highlighted. The secondary structural elements refer to the PSI domain from the Met receptor. The disulfide pairing is shown at the bottom of the figure and colored according to Fig. 1C. (For interpretation of the references to color in this figure legend, the reader is referred to the web version of this paper.)

or alanine) at position 539. Cys538 and Trp540 are invariant and Cys541 is conserved in most PSI domains. Other than the cysteines, Trp540 is the only other strictly conserved amino acid. This tryptophan contributes to the hydrophobic core of the domain by interacting with Leu562. This interaction explains the frequent presence of a hydrophobic residue at position 562. The side chain of Trp540 is located close to the side chains of Cys526, Cys529, and Cys545, suggesting that this tryptophan is invariant because it participates in the folding of PSI domains, sequestering cysteine residues into forming correct disulfide pairing.

Other amino acids in the hydrophobic core include Phe523 and Leu530 that directly interact with each other. Finally, the last well-conserved hydrophobic amino acid, Trp556 in the Met receptor, is only partially buried, explaining more tolerance for various hydrophobic side chains in this location.

#### Structural comparison of PSI domains in the Met receptor and semaphorin

Despite low sequence identity between the Met and Sema4D PSI domains, striking structural similarity is present for an approximately half of the PSI domain. As a result, the two structures can be superimposed using C $\alpha$  carbons for 20 amino acids with RMSD 1.0 Å (Fig. 3A). This structurally conserved region includes the N-terminal part of the domain (His522–Arg548) and the C-terminal Cys561, involved in a disulfide bridge with Cys526. We will refer to this region as a core

of the PSI domain. In contrast, most of the C-terminal half of the PSI domain is quite different in the two structures. This region has different lengths in various PSI-containing proteins and will be called a variable region in this paper. In both PSI domain structures, the C-terminal half wraps around the core of the domain to end at the fixed position of the C-terminal cysteine.

Comparison of the two structures also identifies different structural roles of the disulfide bridges in the PSI domains. Among the three highly conserved disulfide bonds, two disulfides (Cys520–Cys538 and Cys529–Cys545 in the human Met receptor) keep the structural core together, and the third one (Cys526–Cys561) links the C-terminal cysteine to the core. This way, the distance between the N- and C-termini of the PSI domain is well defined, allowing proper orientation of the neighboring domains. The less conserved fourth disulfide (Cys541–Cys551) links the variable region to the core and is clearly not essential for the overall architecture of the PSI domains.

#### Structural core of the PSI domain contains domain-linking surfaces

The identified PSI core constitutes a wedge between the neighboring propeller and immunoglobulin domains (Fig. 4A). PSI-containing proteins belong to both functionally and structurally related groups of receptors, nearly all of which contain the N-terminal propeller domain and the C-terminal IPT, IG, EGF or TSP domains in their extracellular fragments (Fig. 4B). The structural

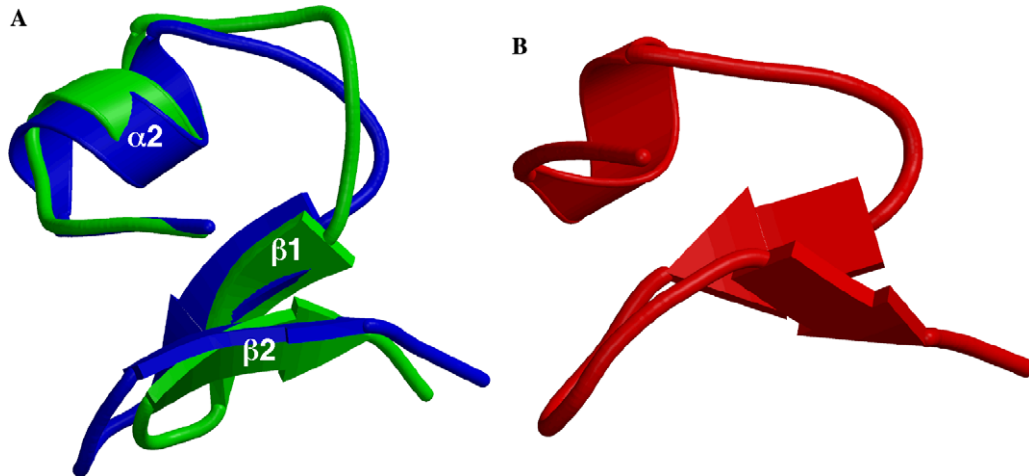


Fig. 3. Structural core of the PSI domain. (A) Backbone superposition of the PSI domain structures from the Met receptor (in green) and Sema4D (PDB code 1OLZ, in blue) using  $C\alpha$  atoms from helix  $\alpha 2$  and strands  $\beta 1$  and  $\beta 2$ . The loops of slightly different lengths were excluded from the superposition. (B) The hanatoxin structure (PDB code 1DIH) is markedly similar to the structural core of the PSI domain. The figure was generated with MOLSCRIPT [21] and Raster3D [22]. (For interpretation of the references to color in this figure legend, the reader is referred to the web version of this paper.)

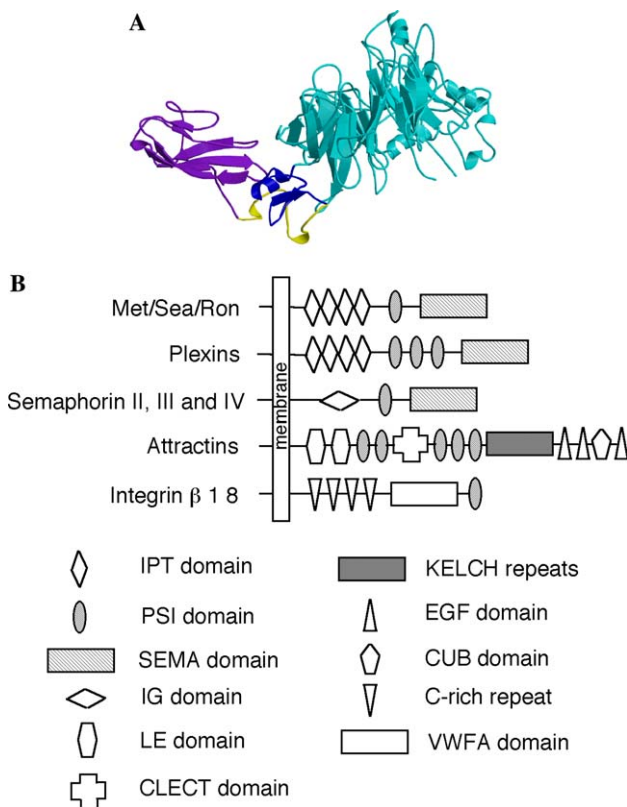


Fig. 4. The PSI domain likely orients the adjacent domains for proper ligand binding. (A) Structurally conserved core of the PSI domain (in blue) in Sema4D (PDB code 1OLZ) links the IG-like domain (in purple) with the propeller-shaped SEMA domain (in cyan). Variable part of the PSI domain is shown in yellow. (B) Schematic representation of extracellular parts of representative PSI-containing receptors. The PSI domain is often positioned between a propeller-like domain and IG-like domain. (For interpretation of the references to color in this figure legend, the reader is referred to the web version of this paper.)

conservation of the core of PSI domains suggests that the interaction interface of the PSI domain may be shared by different members of that class of proteins. The regions of proposed interactions are highlighted in Fig. 2. The IPT-interacting area includes the N-terminal helical region centered between Ser525 and Ser531. By similarity with Sema4D, the contact between the PSI and propeller domains would involve primarily the loops before the first and after the second  $\beta$ -strand (Pro533–Gln537 and Arg547–Glu549 in the human Met receptor). Interestingly, the former has an extension in MEGF8 receptors, which would protrude into the propeller domain. However, these extensions are only present when several PSI domains are in tandem and are observed only in the central domains where they would not collide with the neighboring domains.

#### Similarity of the PSI domain structure to hanatoxin

The conserved core of the PSI domain has a topology similar to those of small toxins represented by hanatoxin (Fig. 3B). Similar to the PSI domain, two disulfide bonds Cys9–Cys21 and Cys15–Cys28 link the helical fragment of hanatoxin with the  $\beta$ -sheet in a similar cross-over fashion. However, the exact position of the disulfides and the helical conformation are slightly different, resulting in a RMSD for  $C\alpha$  atoms above 3 Å between the two structures. Though it was suggested that the sequence similarity between hanatoxin and the semaphorin PSI domains might have functional implications [11], structure-based sequence alignment indicates that the conserved sequence is positioned differently. For instance, the absolutely conserved tryptophan (Trp540 in the PSI domain from Met) is located in the middle of the first  $\beta$ -strand in PSI domains and is partially buried,

while it is positioned at the end of the second  $\beta$ -strand and is solvent-exposed in hanatoxin.

## Discussion

The models of the SEMA domain and the IPT/IG domains of the ectodomain of the Met receptor have been recently proposed based on the deletion mutagenesis and sequence similarity to homologous domains in other structures [19]. This work defines the solution structure of the PSI domain from the Met receptor, providing the structural information on the last missing segment of the ectodomain. It also gives the first detailed structural analysis for this domain, commonly occurring in a wide variety of receptors.

The Met PSI domain structure supports the disulfide pairing found in the Sema4D structure [6], suggesting that this is a general, conserved pattern for PSI domains. The structurally determined disulfide pattern is completely different from that based on the biochemical data for integrins [14]. Uncommonly for the PSI family, the PSI domains of integrins contain seven cysteines and clearly warrant further structural studies. They likely constitute a distinct subclass of the PSI domains, for which larger structural divergence may be expected. For the remaining PSI domains, their fold can be confidently predicted based on the new structural data.

This work demonstrates striking similarity of the structural core of the PSI domains from the Met receptor and semaphorin 4D despite the low amino acid sequence identity. Within this core, mutagenesis data for semaphorin 3A [11] included a double mutation (R531A, D532A) in one of the propeller-interacting loops. Importantly, this mutation greatly attenuated Sema3A function in dorsal root ganglion (DRG) axon repelling. The second triple mutation in the PSI domain (Y534A, W537A, and D538A) also affected the activity of semaphorin. The latter mutation included amino acids from the hydrophobic core of the PSI domain and likely compromised the structure of the domain. Nevertheless, these functional data point to the importance of the PSI domains and their interactions with neighboring domains. The domain-linking surfaces in the PSI domains provide a basis for future mutant design, which should contribute to our understanding of the role of these protein modules in extracellular fragments of plexins, semaphorins, attractins, and other receptors from this class.

## Acknowledgments

K.G. is a Senior Boursier of the FRSQ. This study was supported by the CIHR Grant 14219 to K.G. NRC publication No. 46200.

## References

- [1] L. Trusolino, P.M. Comoglio, Scatter-factor and semaphorin receptors: cell signalling for invasive growth, *Nat. Rev. Cancer* 2 (2002) 289–300.
- [2] C. Birchmeier, W. Birchmeier, E. Gherardi, G.F. Vande Woude, Met, metastasis, motility and more, *Nat. Rev. Mol. Cell. Biol.* 4 (2003) 915–925.
- [3] A. Danilkovitch-Miagkova, B. Zbar, Dysregulation of Met receptor tyrosine kinase activity in invasive tumors, *J. Clin. Invest.* 109 (2002) 863–867.
- [4] S. Rong, S. Segal, M. Anver, J.H. Resau, G.F. Vande Woude, Invasiveness and metastasis of NIH 3T3 cells induced by Met-hepatocyte growth factor/scatter factor autocrine stimulation, *Proc. Natl. Acad. Sci. USA* 91 (1994) 4731–4735.
- [5] A. Antipenko, J.P. Himanen, K. van Leyen, V. Nardi-Dei, J. Lesniak, W.A. Barton, K.R. Rajashankar, M. Lu, C. Hoemme, A.W. Puschel, D.B. Nikolov, Structure of the semaphorin-3A receptor binding module, *Neuron* 39 (2003) 589–598.
- [6] C.A. Love, K. Harlos, N. Mavaddat, S.J. Davis, D.I. Stuart, E.Y. Jones, R.M. Esnouf, The ligand-binding face of the semaphorins revealed by the high-resolution crystal structure of SEMA4D, *Nat. Struct. Biol.* 10 (2003) 843–848.
- [7] P. Bork, T. Doerks, T.A. Springer, B. Snel, Domains in plexins: links to integrins and transcription factors, *Trends Biochem. Sci.* 24 (1999) 261–263.
- [8] J.P. Xiong, T. Stehle, B. Diefenbach, R. Zhang, R. Dunker, D.L. Scott, A. Joachimiak, S.L. Goodman, M.A. Arnaout, Crystal structure of the extracellular segment of integrin alpha Vbeta3, *Science* 294 (2001) 339–345.
- [9] W. Chien, L. Pei, A novel binding factor facilitates nuclear translocation and transcriptional activation function of the pituitary tumor-transforming gene product, *J. Biol. Chem.* 275 (2000) 19422–19427.
- [10] F. Skouri, J. Cohen, Genetic approach to regulated exocytosis using functional complementation in *Paramecium*: identification of the ND7 gene required for membrane fusion, *Mol. Biol. Cell* 8 (1997) 1063–1071.
- [11] O. Behar, K. Mizuno, M. Badminton, C.J. Woolf, Semaphorin 3A growth cone collapse requires a sequence homologous to tarantula hanatoxin, *Proc. Natl. Acad. Sci. USA* 96 (1999) 13501–13505.
- [12] J.P. Xiong, T. Stehle, R. Zhang, A. Joachimiak, M. Frech, S.L. Goodman, M.A. Arnaout, Crystal structure of the extracellular segment of integrin alpha Vbeta3 in complex with an Arg-Gly-Asp ligand, *Science* 296 (2002) 151–155.
- [13] J. Stamos, R.A. Lazarus, X. Yao, D. Kirchhofer, C. Wiesmann, Crystal structure of the HGF beta-chain in complex with the Sema domain of the Met receptor, *EMBO J.* 27 (2004) [Epub ahead of print].
- [14] J.J. Calvete, A. Henschen, J. Gonzalez-Rodriguez, Assignment of disulphide bonds in human platelet GPIIIa. A disulphide pattern for the beta-subunits of the integrin family, *Biochem. J.* 274 (1991) 63–71.
- [15] C. Bartels, T.-H. Xia, M. Billeter, P. Guntert, K. Wuthrich, The program XEASY for computer-supported NMR spectral analysis of biological macromolecules, *J. Biomol. NMR* 5 (1995) 1–10.
- [16] T. Herrmann, P. Guntert, K. Wuthrich, Protein NMR structure determination with automated NOE assignment using the new software CANDID and the torsion angle dynamics algorithm DYANA, *J. Mol. Biol.* 319 (2002) 209–227.
- [17] C.D. Schwieters, J.J. Kuszewski, N. Tjandra, G.M. Clore, The Xplor-NIH NMR molecular structure determination package, *J. Magn. Res.* 160 (2003) 66–74.

- [18] R.A. Laskowski, J.A. Rullmann, M.W. MacArthur, R. Kaptein, J.M. Thornton, AQUA and PROCHECK-NMR: programs for checking the quality of protein structures solved by NMR, *J. Biomol. NMR* 8 (1996) 477–486.
- [19] E. Gherardi, M.E. Youles, R.N. Miguel, T.L. Blundell, L. Iamele, J. Gough, A. Bandyopadhyay, G. Hartmann, P.J. Butler, Functional map and domain structure of MET, the product of the c-met protooncogene and receptor for hepatocyte growth factor/scatter factor, *Proc. Natl. Acad. Sci. USA* 100 (2003) 12039–12044.
- [20] R. Koradi, M. Billeter, K. Wuthrich, MOLMOL: a program for display and analysis of macromolecular structures, *J. Mol. Graph.* 14 (1996) 51–55.
- [21] P.J. Kraulis, MOLSCRIPT: a program to produce both detailed and schematic plots of protein structures, *J. Appl. Cryst.* 24 (1991) 946–950.
- [22] E.A. Merritt, M.E.P. Murphy, Raster3D version 2.0: a program for photorealistic molecular graphics, *Acta Crystallogr. D* 50 (1994) 869–873.